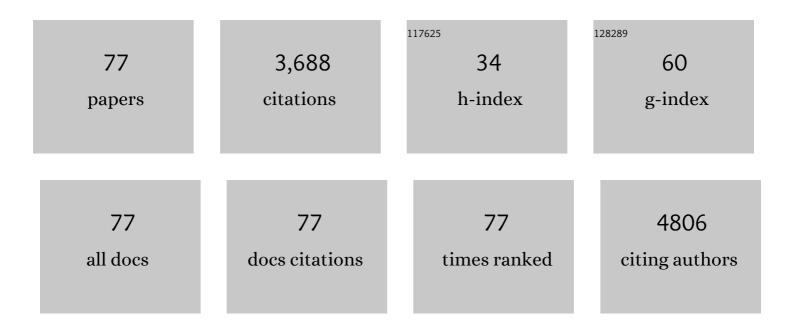
Chun-Yan Wu

List of Publications by Year in descending order

Source: https://exaly.com/author-pdf/379727/publications.pdf Version: 2024-02-01



<u> Chun-Yan Wu</u>

#	Article	IF	CITATIONS
1	Highly reliable Cu Cu low temperature bonding using SAC305 solder with rGO interlayer. Microelectronics Reliability, 2022, 129, 114483.	1.7	3
2	Grating Perovskite Enhanced Polarization-Sensitive GaAs-Based Photodetector. IEEE Transactions on Electron Devices, 2022, 69, 2469-2473.	3.0	5
3	A quasi-2D perovskite antireflection coating to boost the performance of multilayered PdTe ₂ /Ge heterostructure-based near-infrared photodetectors. Journal of Materials Chemistry C, 2022, 10, 6025-6035.	5.5	5
4	Spectral Engineering of InSe Nanobelts for Full-Color Imaging by Tailoring the Thickness. Journal of Physical Chemistry Letters, 2022, 13, 2668-2673.	4.6	3
5	Wavelength-Tunable Multispectral Photodetector With Both Ultraviolet and Near-Infrared Narrowband Detection Capability. IEEE Transactions on Electron Devices, 2022, 69, 3258-3261.	3.0	5
6	Nonâ€Ultrawide Bandgap Semiconductor GaSe Nanobelts for Sensitive Deep Ultraviolet Light Photodetector Application. Small, 2022, 18, e2200594.	10.0	13
7	Ultraviolet Photodetectors Based on Nanometer-Thick Films of the Narrow Band Gap Semiconductor PbS. ACS Applied Nano Materials, 2022, 5, 8894-8901.	5.0	1
8	Fabrication of Addressable Perovskite Film Arrays for High-Performance Photodetection and Real-Time Image Sensing Application. Journal of Physical Chemistry Letters, 2021, 12, 2930-2936.	4.6	23
9	Nanochannel-confined growth of crystallographically orientated perovskite nanowire arrays for polarization-sensitive photodetector application. Science China Materials, 2021, 64, 2497-2506.	6.3	21
10	Enhanced Light Trapping in Conformal CuO/Si Microholes Array Heterojunction for Self-Powered Broadband Photodetection. IEEE Electron Device Letters, 2021, 42, 883-886.	3.9	7
11	Multilayered PdTeâ,,/GaN Heterostructures for Visible-Blind Deep-Ultraviolet Photodetection. IEEE Electron Device Letters, 2021, 42, 1192-1195.	3.9	18
12	Multilayered PtSe ₂ /pyramid-Si heterostructure array with light confinement effect for high-performance photodetection, image sensing and light trajectory tracking applications. Journal of Materials Chemistry C, 2021, 9, 2823-2832.	5.5	20
13	Electrically adjusted deep-ultraviolet/near-infrared single-band/dual-band imaging photodetectors based on Cs ₃ Cu ₂ I ₅ /PdTe ₂ /Ge multiheterostructures. Journal of Materials Chemistry C, 2021, 9, 14897-14907.	5.5	14
14	Probing the trap states in N–i–P Sb2(S,Se)3 solar cells by deep-level transient spectroscopy. Journal of Chemical Physics, 2020, 153, 124703.	3.0	16
15	High-performance light trajectory tracking and image sensing devices based on a γ-In ₂ Se ₃ /GaAs heterostructure. Journal of Materials Chemistry C, 2020, 8, 13762-13769.	5.5	11
16	Efficient defect passivation of Sb ₂ Se ₃ film by tellurium doping for high performance solar cells. Journal of Materials Chemistry A, 2020, 8, 6510-6516.	10.3	48
17	Water Additive Enhanced Solution Processing of Alloy Sb ₂ (S _{1â^²<i>x</i>} Se _{<i>x</i>}) ₃ â€Based Solar Cells. Solar Rrl, 2020, 4, 1900582.	5.8	38
18	Controlled synthesis of GaSe microbelts for high-gain photodetectors induced by the electron trapping effect. Journal of Materials Chemistry C, 2020, 8, 5375-5379.	5.5	12

#	Article	IF	CITATIONS
19	Pulsed laser deposition of antimony selenosulfide thin film for efficient solar cells. Applied Physics Letters, 2020, 116, .	3.3	16
20	Self-Powered Filterless Narrow-Band p–n Heterojunction Photodetector for Low Background Limited Near-Infrared Image Sensor Application. ACS Applied Materials & Interfaces, 2020, 12, 21845-21853.	8.0	37
21	Cu-Cu low temperature bonding based on lead-free solder with graphene interlayer. Applied Physics Letters, 2019, 115, .	3.3	8
22	Catalystâ€Free Vapor–Solid Deposition Growth of βâ€Ga ₂ O ₃ Nanowires for DUV Photodetector and Image Sensor Application. Advanced Optical Materials, 2019, 7, 1901257.	7.3	62
23	Defect-induced broadband photodetection of layered γ-In ₂ Se ₃ nanofilm and its application in near infrared image sensors. Journal of Materials Chemistry C, 2019, 7, 11532-11539.	5.5	36
24	Opening the Band Gap of Graphene via Fluorination for High-Performance Dual-Mode Photodetector Application. ACS Applied Materials & Interfaces, 2019, 11, 21702-21710.	8.0	28
25	Asymmetric Contactâ€Induced Selfâ€Driven Perovskiteâ€Microwireâ€Array Photodetectors. Advanced Electronic Materials, 2019, 5, 1900135.	5.1	40
26	A high-performance near-infrared light photovoltaic detector based on a multilayered PtSe ₂ /Ge heterojunction. Journal of Materials Chemistry C, 2019, 7, 5019-5027.	5.5	58
27	Grapheneâ€Assisted Growth of Patterned Perovskite Films for Sensitive Light Detector and Optical Image Sensor Application. Small, 2019, 15, e1900730.	10.0	53
28	Thickness-Dependent Resistive Switching Behavior of KCu ₇ S ₄ /Cu _{<i>x</i>} O/Au Device. Journal of Nanoscience and Nanotechnology, 2019, 19, 2844-2850.	0.9	8
29	Transforming ground mica into high-performance biomimetic polymeric mica film. Nature Communications, 2018, 9, 2974.	12.8	107
30	Self-assembled KCu ₇ S ₄ nanowire monolayers for self-powered near-infrared photodetectors. Nanoscale, 2018, 10, 18502-18509.	5.6	15
31	Controllable synthesis of p-type Cu2S nanowires for self-driven NIR photodetector application. Journal of Nanoparticle Research, 2017, 19, 1.	1.9	10
32	Design and construction of ultra-thin MoSe2 nanosheet-based heterojunction for high-speed and low-noise photodetection. Nano Research, 2016, 9, 2641-2651.	10.4	43
33	A top-down strategy to synthesize wurtzite Cu ₂ ZnSnS ₄ nanocrystals by green chemistry. Chemical Communications, 2016, 52, 9821-9824.	4.1	12
34	Core–shell silicon nanowire array–Cu nanofilm Schottky junction for a sensitive self-powered near-infrared photodetector. Journal of Materials Chemistry C, 2016, 4, 10804-10811.	5.5	32
35	Facial synthesis of KCu ₇ S ₄ nanobelts for nonvolatile memory device applications. Journal of Materials Chemistry C, 2016, 4, 589-595.	5.5	12
36	Preparation and Photoelectric and Magnetic Properties of Cu ₂ MnSnS ₄ Nanosheets. ChemPlusChem, 2015, 80, 1537-1540.	2.8	4

#	Article	IF	CITATIONS
37	In Situ Carbon-Doped Mo(Se _{0.85} S _{0.15}) ₂ Hierarchical Nanotubes as Stable Anodes for High-Performance Sodium-Ion Batteries. Small, 2015, 11, 5667-5674.	10.0	101
38	Surface charge transfer induced p-CdS nanoribbon/n-Si heterojunctions as fast-speed self-driven photodetectors. Journal of Materials Chemistry C, 2015, 3, 6307-6313.	5.5	24
39	p-type ZnTe:Ca nanowires: controlled doping and optoelectronic device application. RSC Advances, 2015, 5, 13324-13330.	3.6	20
40	Core–shell CdS:Ga–ZnTe:Sb p–n nano-heterojunctions: fabrication and optoelectronic characteristics. Journal of Materials Chemistry C, 2015, 3, 2933-2939.	5.5	8
41	Water Evaporation Induced Conversion of CuSe Nanoflakes to Cu _{2â^'<i>x</i>} Se Hierarchical Columnar Superstructures for High-Performance Solar Cell Applications. Particle and Particle Systems Characterization, 2015, 32, 840-847.	2.3	34
42	Interfacial state induced ultrasensitive ultraviolet light photodetector with resolved flux down to 85 photons per second. Nano Research, 2015, 8, 1098-1107.	10.4	17
43	The Effect of Plasmonic Nanoparticles on the Optoelectronic Characteristics of CdTe Nanowires. Small, 2014, 10, 2645-2652.	10.0	43
44	Gallium doped <i>n</i> -type Zn _x Cd _{1-x} S nanoribbons: Synthesis and photoconductivity properties. Journal of Applied Physics, 2014, 115, 063108.	2.5	8
45	n-Type KCu ₃ S ₂ microbelts: optical, electrical, and optoelectronic properties. RSC Advances, 2014, 4, 59221-59225.	3.6	6
46	Nearâ€Infrared Light Photovoltaic Detector Based on GaAs Nanocone Array/Monolayer Graphene Schottky Junction. Advanced Functional Materials, 2014, 24, 2794-2800.	14.9	167
47	Core–Shell Heterojunction of Silicon Nanowire Arrays and Carbon Quantum Dots for Photovoltaic Devices and Self-Driven Photodetectors. ACS Nano, 2014, 8, 4015-4022.	14.6	258
48	Interfacially Engineered Highâ€Speed Nonvolatile Memories Employing pâ€Type Nanoribbons. Advanced Materials Interfaces, 2014, 1, 1400130.	3.7	3
49	Light trapping and surface plasmon enhanced high-performance NIR photodetector. Scientific Reports, 2014, 4, 3914.	3.3	132
50	Monolayer Graphene/Germanium Schottky Junction As High-Performance Self-Driven Infrared Light Photodetector. ACS Applied Materials & Interfaces, 2013, 5, 9362-9366.	8.0	347
51	High-speed ultraviolet-visible-near infrared photodiodes based on p-ZnS nanoribbon–n-silicon heterojunction. CrystEngComm, 2013, 15, 1635.	2.6	27
52	Tuning the p-type conductivity of ZnSe nanowiresvia silver doping for rectifying and photovoltaic device applications. Journal of Materials Chemistry A, 2013, 1, 1148-1154.	10.3	29
53	Flexible CuS nanotubes–ITO film Schottky junction solar cells with enhanced light harvesting by using an Ag mirror. Nanotechnology, 2013, 24, 045402.	2.6	16
54	Monolayer Graphene Film on ZnO Nanorod Array for Highâ€Performance Schottky Junction Ultraviolet Photodetectors. Small, 2013, 9, 2872-2879.	10.0	271

#	Article	IF	CITATIONS
55	Ultrahigh Mobility of pâ€Type CdS Nanowires: Surface Charge Transfer Doping and Photovoltaic Devices. Advanced Energy Materials, 2013, 3, 579-583.	19.5	37
56	p-type ZnS:N nanowires: Low-temperature solvothermal doping and optoelectronic properties. Applied Physics Letters, 2013, 103, 213111.	3.3	21
57	Surface charge transfer doping of germanium nanowires by MoO3 deposition. RSC Advances, 2012, 2, 3361.	3.6	7
58	Self-powered and fast-speed photodetectors based on CdS:Ga nanoribbon/Au Schottky diodes. Journal of Materials Chemistry, 2012, 22, 23272.	6.7	116
59	Transparent and flexible selenium nanobelt-based visible light photodetector. CrystEngComm, 2012, 14, 1942.	2.6	68
60	Device structure-dependent field-effect and photoresponse performances of p-type ZnTe:Sb nanoribbons. Journal of Materials Chemistry, 2012, 22, 6206.	6.7	96
61	p-CdTe nanoribbon/n-silicon nanowires array heterojunctions: photovoltaic devices and zero-power photodetectors. CrystEngComm, 2012, 14, 7222.	2.6	38
62	Aluminium-doped n-type ZnS nanowires as high-performance UV and humidity sensors. Journal of Materials Chemistry, 2012, 22, 6856.	6.7	79
63	Schottky solar cells based on graphene nanoribbon/multiple silicon nanowires junctions. Applied Physics Letters, 2012, 100, 193103.	3.3	65
64	Chlorineâ€Ðoped ZnSe Nanoribbons with Tunable nâ€Type Conductivity as Highâ€Gain and Flexible Blue/UV Photodetectors. ChemPlusChem, 2012, 77, 470-475.	2.8	15
65	Tailoring the electrical properties of tellurium nanowires via surface charge transfer doping. Journal of Nanoparticle Research, 2012, 14, 1.	1.9	13
66	High-gain visible-blind UV photodetectors based on chlorine-doped n-type ZnS nanoribbons with tunable optoelectronic properties. Journal of Materials Chemistry, 2011, 21, 12632.	6.7	64
67	Monolayer graphene film/silicon nanowire array Schottky junction solar cells. Applied Physics Letters, 2011, 99, .	3.3	120
68	Surface induced negative photoconductivity in p-type ZnSe : Bi nanowires and their nano-optoelectronic applications. Journal of Materials Chemistry, 2011, 21, 6736.	6.7	89
69	Synthesis and optoelectronic properties of silver-doped n-type CdS nanoribbons. Frontiers of Optoelectronics in China, 2011, 4, 161-165.	0.2	4
70	Nano-Schottky barrier diodes based on Sb-doped ZnS nanoribbons with controlled p-type conductivity. Applied Physics Letters, 2011, 98, .	3.3	35
71	High-performance CdS:P nanoribbon field-effect transistors constructed with high-κ dielectric and top-gate geometry. Applied Physics Letters, 2010, 96, .	3.3	41
72	Chlorine-doped n-type CdS nanowires with enhanced photoconductivity. Nanotechnology, 2010, 21, 505203.	2.6	66

#	Article	IF	CITATIONS
73	Tectonic arrangement of Bi2S3 nanocrystals into 2D networks. Journal of Materials Chemistry, 2009, 19, 3378.	6.7	38
74	Three-dimensional imaging of a complex concaved cuboctahedron copper sulfide crystal by x-ray nanotomography. Applied Physics Letters, 2008, 92, .	3.3	41
75	Large scale synthesis of uniform CuS nanotubes in ethylene glycol by a sacrificial templating method under mild conditions. Journal of Materials Chemistry, 2006, 16, 3326.	6.7	178
76	Complex Concaved Cuboctahedrons of Copper Sulfide Crystals with Highly Geometrical Symmetry Created by a Solution Process. Chemistry of Materials, 2006, 18, 3599-3601.	6.7	98
77	Fabrication of a γ-In ₂ Se ₃ /Si heterostructure phototransistor for heart rate detection. Journal of Materials Chemistry C, 0, , .	5.5	4